MICROCOPY RESOLUTION TEST CHART

NATIONAL BUREAU OF STANDARDS-1963-A

Report PME-FM 87-1

INJECTION OF DRAG REDUCING ADDITIVES INTO TURBULENT WATER FLOWS

Mixing Experiments and Newtonian Burst Frequency

William G. Tiederman, David T. Walker, and C. David Bustetter
School of Mechanical Engineering
Purdue University
West Lafayette, Indiana 47907

DTIC
ELECTE
S
D
JUN 0 3 1987
D

April 1987

Technical Report for Period 01 March 1986 - 28 February 1987

Prepared for

87   6   2   005

REPORT DOCUMENTATION PAGE		READ INSTRUCTIONS BEFORE COMPLETING FORM
1. REPORT NUMBER PME-FM-87-1	2. GOVT ACCESSION NO.	3. RECIPIENT'S CATALOG NUMBER
4. TITLE *(and Subtitle)* INJECTION OF DRAG REDUCING ADDITIVES INTO TURBULENT WATER FLOWS: Mixing Experiments and Newtonian Burst Frequency		5. TYPE OF REPORT & PERIOD COVERED Annual Report for March 1, 1986 through February 28, 1987
		6. PERFORMING ORG. REPORT NUMBER
7. AUTHOR(s) William G. Tiederman, David T. Walker and C. David Bustetter		8. CONTRACT OR GRANT NUMBER(s) N00014-83K-0183
9. PERFORMING ORGANIZATION NAME AND ADDRESS School of Mechanical Engineering Purdue University West Lafayette, Indiana 47907		10. PROGRAM ELEMENT, PROJECT, TASK AREA & WORK UNIT NUMBERS NR 4322754
11. CONTROLLING OFFICE NAME AND ADDRESS Office of Naval Research 800 North Quincy Street Arlington, VA 22217-5000		12. REPORT DATE April 1987
		13. NUMBER OF PAGES 42
14. MONITORING AGENCY NAME & ADDRESS(If different from Controlling Office)		15. SECURITY CLASS. (of this report)
		15a. DECLASSIFICATION/DOWNGRADING SCHEDULE

16. DISTRIBUTION STATEMENT (of this Report)

APPROVED FOR PUBLIC RELEASE: DISTRIBUTION UNLIMITED

17. DISTRIBUTION STATEMENT (of the abstract entered in Block 30, if different from Report)

18. SUPPLEMENTARY NOTES

19. KEY WORDS (Continue on reverse side if necessary and identify by block number)

Drag reduction; turbulent wall flows; concentration measurements

20. ABSTRACT (Continue on reverse side if necessary and identify by block number)

The basic goals of this project are to determine the mechanisms by which drag-reducing aditives modify the turbulent transport near walls and to develop optimum methods for injecting these additives into flows of water. The purpose is to develop methods for controlling and manipulating turbulent wall flows.

DD FORM 1473 EDITION OF 1 NOV 65 IS OBSOLETE
1 JAN 73
S/N 0102-014-6601 |

20. Abstract (continued)

This first portion of the report describes two-component velocity measurements and mean concentration measurements in the region where a concentrated, drag-reducing, additive solution mixes with a channel flow of water. The additive is introduced through flush mounted, angled injectors that initially place the solution next to the wall. Near the injectors, the mean concentration profiles contain very sharp gradients that separate high concentration wall regions from a low concentration core. When the central core is void of additive the root-mean-square of the normal velocity fluctuation, v', and the Reynolds shear stress, $\rho \overline{uv}$, are unaffected in this core region. These two quantities are significantly lower in the high concentration, wall region compared to their corresponding water flow levels. Further downstream, where the additive is present across the entire channel, v' and $\rho \overline{uv}$ are reduced across the entire channel. This indicates that once the additive has mixed beyond the wall region in even small quantities the structure of the flow is altered everywhere.

The second portion of the report describes single component laser velocimeter measurements in a Newtonian channel flow where the Reynolds number was 50,000. The purpose of these measurements was to deduce the average time between bursts at this relatively high Reynolds number. The results show that the time between bursts when scaled with wall shear velocity and kinematic viscosity has a constant value of 90 for the Reynolds number range 9,400 to 50,000.

TABLE OF CONTENTS

Page No.

1. INTRODUCTION

The basic goals of this project are to determine the mechanisms by which drag-reducing additives modify the turbulent transport near walls and to develop optimum methods for injecting these additives into wall bounded flows of water. The purpose is to develop methods for predicting, controlling and manipulating turbulent wall flows.

The addition of small amounts of soluble, high molecular weight polymer molecules to water flows has been one of the most successful methods for reducing drag and manipulating the near-wall, turbulent structure. There are two variations in the basic technique. In the original method, relatively low concentrations of the additive were injected and the additive mixed at the molecular level with the water flow. Recently, Bewersdorff (1985), Frings (1985) and Berman (1986) have reported results for flows where more concentrated solutions were injected and the resulting flow contained one large or many small threads of concentrated polymer solution. Currently, this project is concerned only with the original technique where solutions with concentrations less than 0.2% are injected through flush mounted, angled wall slots into fully developed channel flows of water (see Walker et al., 1986).

Two somewhat different technical issues have been addressed during this past year. The major portion of this report will describe the evolution of the time-average concentration profiles and velocity statistics downstream of the optimal injection process described by Walker et al. (1986). Additive concentration was deduced from an optical attenuation technique when the injected material was marked with dye. Velocity data were obtained with a two-color, two-component laser velocimeter aligned to measure simultaneously the velocity components in the streamwise and wall normal

directions. These data describe the velocity and concentration profiles at four, eight, sixteen and thirty-two channel heights downstream of the injectors. At the upstream position the additive is primarily confined to a region near the wall. At the downstream position the additive is well mixed throughout the channel flow.

The other technical issue centers on the time scale associated with the near-wall turbulent structure (the time between bursts). In a Newtonian flow, essentially all of the turbulent kinetic energy and most of the turbulent transport occurs during the burst events (see Corino and Bradkey, 1969 and Kim et al., 1971). The burst event is a sudden outrush of low momentum fluid away from the wall. Associated with each burst is a sweep or inrush of high momentum fluid toward the wall. Since the burst event is associated with major velocity fluctuations in the near-wall region where drag-reducing solutions have an effect on the time-average flow field, the changes that take place in the burst events in drag-reducing flows are of particular interest. The burst data reported here were acquired at a Reynolds Number of 50,000 to confirm the inner variable scaling discussed by Luchik and Tiederman (1987) for Newtonian flows and are needed before further comparisons with drag-reducing measurements are made.

2. MIXING EXPERIMENTS

These initial experiments were conducted to demonstrate the feasibility of the techniques and to determine the evolution of the mean polymer concentration profile and turbulent velocity statistics downstream of a wall injection of a polymer solution. These experiments will serve as a guide in the design of more detailed experiments that will follow.

2.1 Apparatus and Procedures

The test section of the recirculating water flow loop used in these experiments was the 2.5 cm high by 25 cm wide rectangular cross-section channel described by Walker et al. (1986). The channel was constructed from one half inch acrylic sheet and is more than one hundred channel heights long. Polymer solutions are injected through flush-mounted, angled slots located in both long walls of the channel. The average slot angle is 25˚ with respect to the wall and the streamwise width at the wall is 0.100 inches. The injectors are located more than one hundred channel heights downstream of the inlet.

The flow loop is driven by four ninety gallon per minute centrifugal pumps operating in parallel. At each end of the test section there is a large stilling tank to isolate the test section from any hydrodynamic disturbances in the flow loop. The upstream stilling tank contains a perforated plate followed by screen and open-cell sponge section and a smooth two-dimensional contraction at the outlet. The inlet of the channel is preceded by a flow straightener consisting of closely packed plastic drinking straws which insures that no large-scale vorticity exists in the channel entry

flow. The downstream tank contains a perforated plate to damp out disturbances and a copper coil through which cooling water is passed to maintain the channel water at a constant temperature.

The reduction in wall shear stress which occurs during polymer injection, was deduced in two ways. If the flow is approximately fully developed, then the wall shear stress is proportional to the pressure drop and the fractional reduction in pressure drop resulting from polymer injection is equal to the drag reduction. Static pressure drop measurements were made with Gilmont micromanometers using carbon tetrachloride as the working fluid. Because the fluid is recirculated with intermittent injection of polymer, the water-flow pressure gradient had to be monitored periodically during an experiment to insure that drag reduction due to polymer accumulating in the flow loop did not occur. These checks showed that once the polymer solution had passed the test section, it was no longer an effective drag reducer.

The second method of deducing drag reduction was by estimating the mean velocity gradient at the wall from near-wall velocity measurements and measuring the mean near-wall polymer concentration. These results were then used, along with viscometric data to determine the wall shear stress directly from

$$\tau_w = \mu \left(\frac{\partial \bar{U}}{\partial y} \right)_w \qquad (1)$$

Two component velocity measurements were made using a Thermo-Systems Incorporated (TSI) model 9100-6 laser velocimeter system incorporating a 500 mW Lexel model 85 Argon-ion laser. This two channel, two color, four beam system was

oriented so that the optical axis was parallel to the long walls of the channel and perpendicular to the flow direction allowing direct measurement of the streamwise and normal velocity components. To allow measurements very near the wall the lower beam of the pair used to measure the normal velocity was displaced to the optical axis. The beams were focused using a 250 mm focal length lens yielding a measurement volume with a diameter of 65 μm and a length of 300 μm.

The scattered radiation was collected in forward scatter slightly off the optical axis. Combining a 250 mm focal length lens and a 130 μm aperture in a TSI model 9143 field stop assembly results in a field of view about 300 μm in diameter for the receiving optics. This results in the effective probe volume length of about 1.1 mm in the spanwise direction.

Both channels of the laser velocimeter were frequency-shifted 40 MHz and the photomultiplier output for each channel was electronically down-mixed to yield a net frequency shift of 0.5 MHz. Velocity information was extracted from the down-mixed photomultiplier output using two TSI model 1980 counter type processors operating in the N-cycle mode. Temporal coincidenced was imposed in the measurements and the data were transferred to a Digital Equipment Corp. PDP 11/03 mini-computer using a TSI model 1998 interface. Data were then transferred to a VAX 11/780 computer for statistical analysis.

In these experiments, velocity measurements were made both in pure water flows and in flows where turbulent fluctuations in the polymer concentration occurred. In order to eliminate bias in the velocity statistics caused by concentration fluctuations, the seed particle concentration in the channel water had to match that in the injected

polymer solution. To accomplish this, the channel water was seeded using fat particles from whole milk so that the particle arrival rate did not change significantly when the polymer injectors were turned on. Ensembles of four thousand points, acquired by making only one measurement per Doppler burst, were used to calculate velocity statistics. The two-dimensional weighting method of Tiederman (1979) was used to correct these ensembles for velocity bias since the sampling rate and the particle arrival rate were correlated.

Mean polymer concentration profiles were measured by dyeing the injected polymer solution with Rhodamine B dye and then measuring the attenuation of a laser beam directed across the span of the channel parallel to the wall when the injectors were turned on. The green (514.5 nm) line of a Lexel model 85 laser was used and the change in the beam intensity was measured using an Oriel model 71841 silicon photodiode. This combination yielded spatial resolution of 0.5 mm in the direction normal to the wall. The logarithm of the intensity change is proportional to the space-averaged dye concentration along the path of the beam. Since the span of the channel was not long enough to result in a temporally constant space-averaged polymer concentration, the output of the photodiode was input to a logarithmic amplifier to obtain a signal that was proportional to the space-averaged concentration along the beam path. This signal was then time averaged using an integrating voltmeter.

Experiments were conducted at a Reynolds number of 18500 based on mass-averaged velocity and channel height in the 2.5 cm channel. This resulted in a shear velocity, u_τ, of 3.79 cm/s. A seven hundred ppm aqueous solution of SEPARAN AP-

273 was injected through the flush-mounted angled injectors at a flowrate equal to that in the undisturbed linear sublayer of the water flow (450 ml/min). Mean polymer concentration measurements were made at locations 4, 8, 16 and 32 channel heights downstream of the injectors. Two-component velocity measurements were made at these same locations both with and without polymer injection.

2.2 Results

Figures 1 through 3 show the first and second statistical moments of the streamwise and normal velocity components normalized with inner variables (shear velocity, $u_r = \sqrt{\tau_w/\rho}$ and kinematic viscosity, ν for the flow without polymer injection) at the four measurement locations. These measurements indicate that the flow was typical of fully-developed, two-dimensional channel flow.

Variation of drag reduction with position downstream of the injector is presented in Figure 4. These data were calculated from both pressure drop and velocity measurements. The drag reduction levels calculated using pressure drop measurements were in reasonable agreement with those obtained by Walker et al. (1986) in the same channel at a Reynolds number of 17,800 and the same injection flowrate and polymer concentration. Comparison of the values of drag reduction calculated from the slope of measured mean velocity profiles at the wall and pressure drop measurements indicates that the pressure drop measurements give a reasonable approximation to the drag-reduction levels calculated from the average wall shear rate.
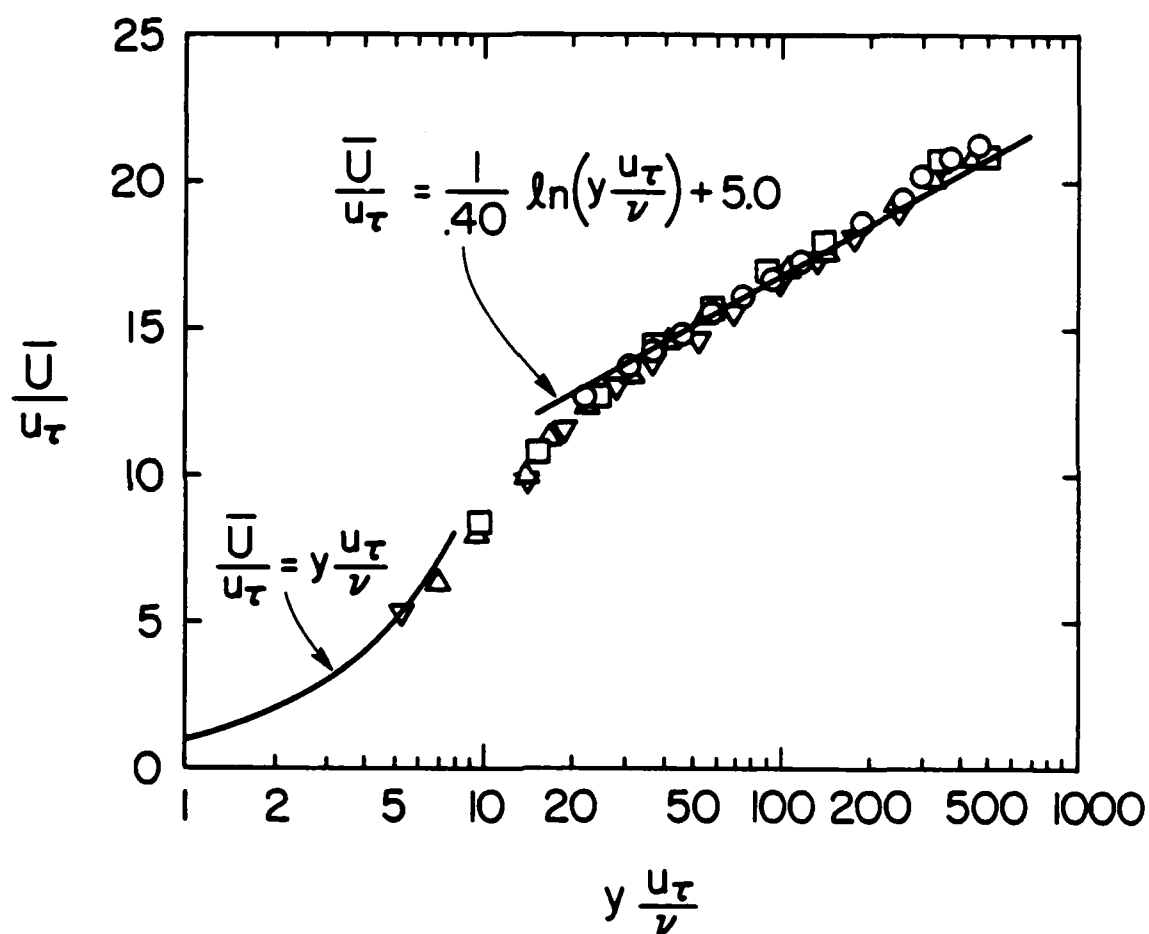
Figure 1.   Mean velocity profiles for water flow; □, x/h = 4; ◯, 8 ; △, 16; ▽, 32.
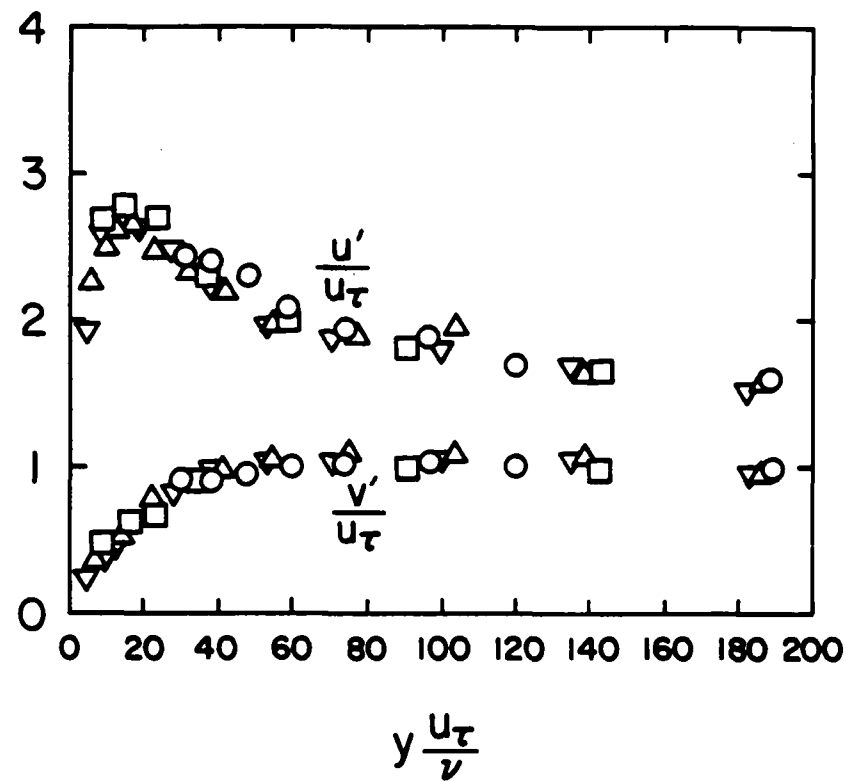
Figure 2.　Root - mean - square streamwise and normal velocity profiles for water flow; □, x/h = 4; ○, 8; △, 16; ▽, 32.
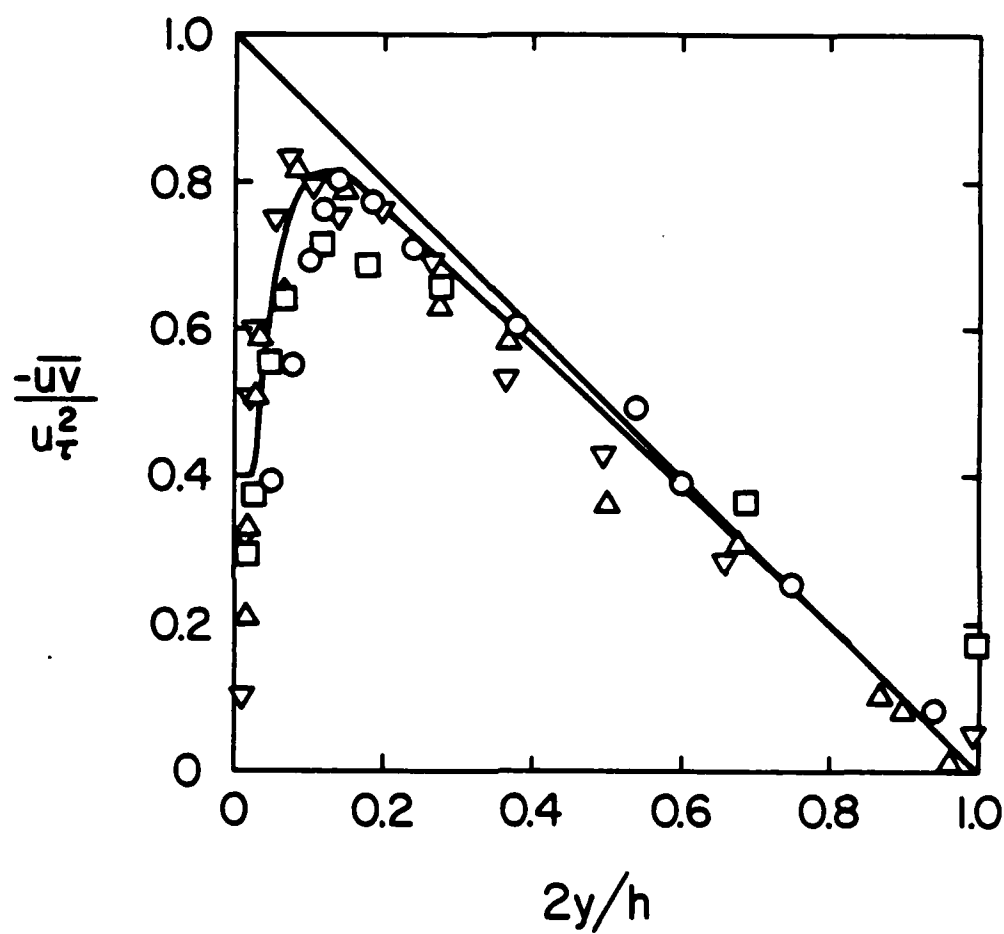
Figure 3.   Turbulent shear stress profiles for water flow; □, x/h = 4;
○, 8; △, 16; ▽, 32; ——, 1 - 2 y/h - dU$^+$/dy$^+$.

Mean polymer concentration profiles are shown in Figure 5 for the four measurement locations. At the near-injector location ($x/h = 4$), the polymer concentration near the wall has been reduced to less than one-third the injected polymer concentration but there is still a sharp gradient between the high concentration near-wall region and the outer flow. The near-wall concentration decreases with increasing distance downstream until the concentration is nearly uniform thirty-two channel heights downstream of the injectors. This result is in agreement with pressure-drop measurements which indicate that drag-reduction is nearly constant downstream of this location.

The flow has reached a near fully-developed condition at the far downstream measurement location ($x/h = 32$) where the level of drag reduction was measured at thirty-four percent. Figures 6 and 7 compare the first and second moments of the streamwise and normal velocity components with those of Luchik (1985) which were made in the same channel with a drag-reduction level of thirty-one percent for a fully-developed flow at a Reynolds number of 22,000. The quantities are normalized with the local (drag-reducing) values of shear velocity and kinematic viscosity. With the exception of the root-mean-square of the normal velocity component, the agreement between these two data sets is very close. While these two flows are only similar in terms of the drag reduction level, this comparison indicates that the flow is approaching a condition that one would expect in a fully developed drag-reducing channel flow.
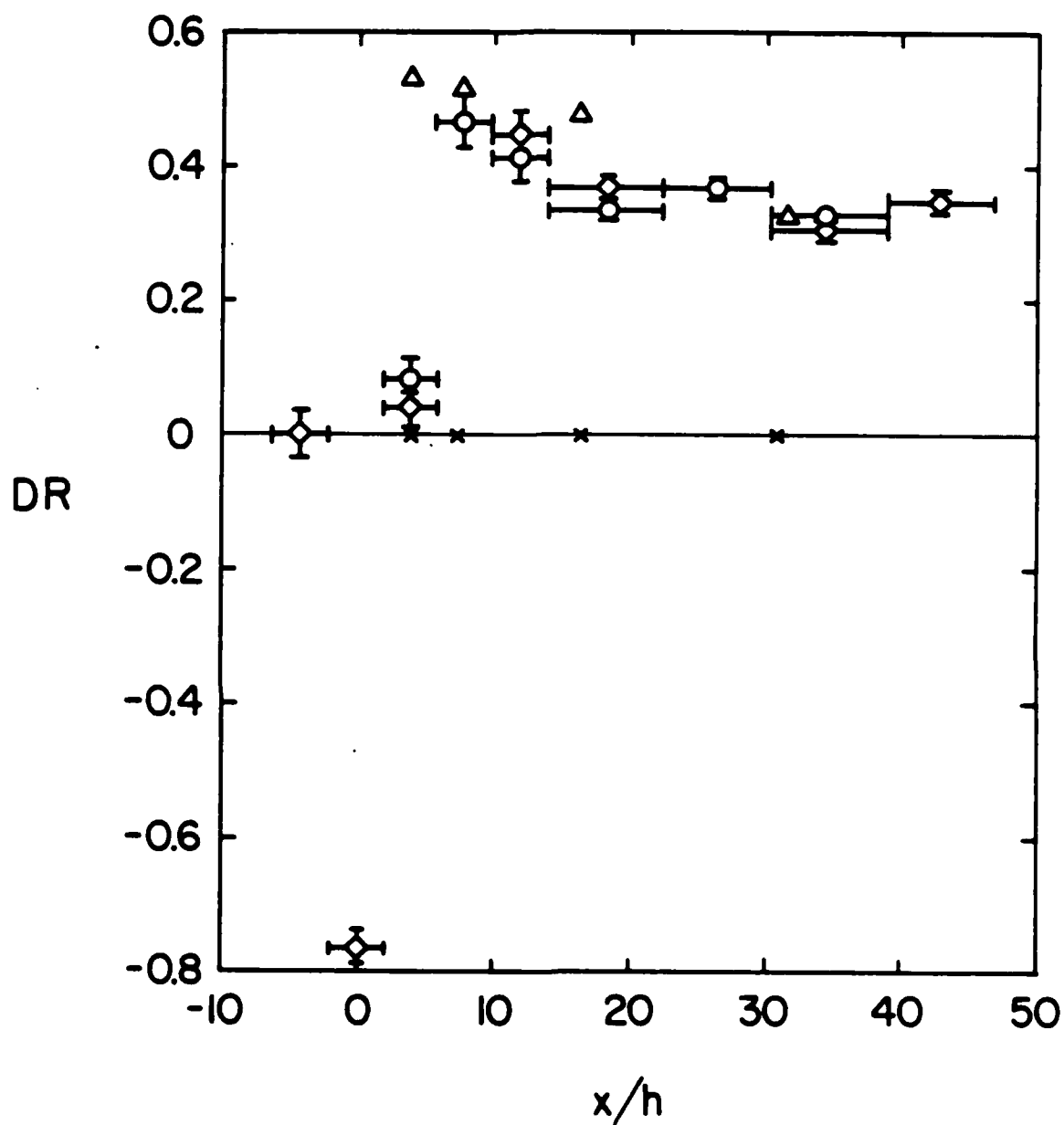
Figure 4.   Variation of drag reduction with streamwise location for an injection of 700 ppm SEPARAN AP-273 at a flowrate of 450 ml/min; $\Diamond$, Walker et al. (1986); $\bigcirc$; present, pressure drop; $\triangle$, present, wall slope.
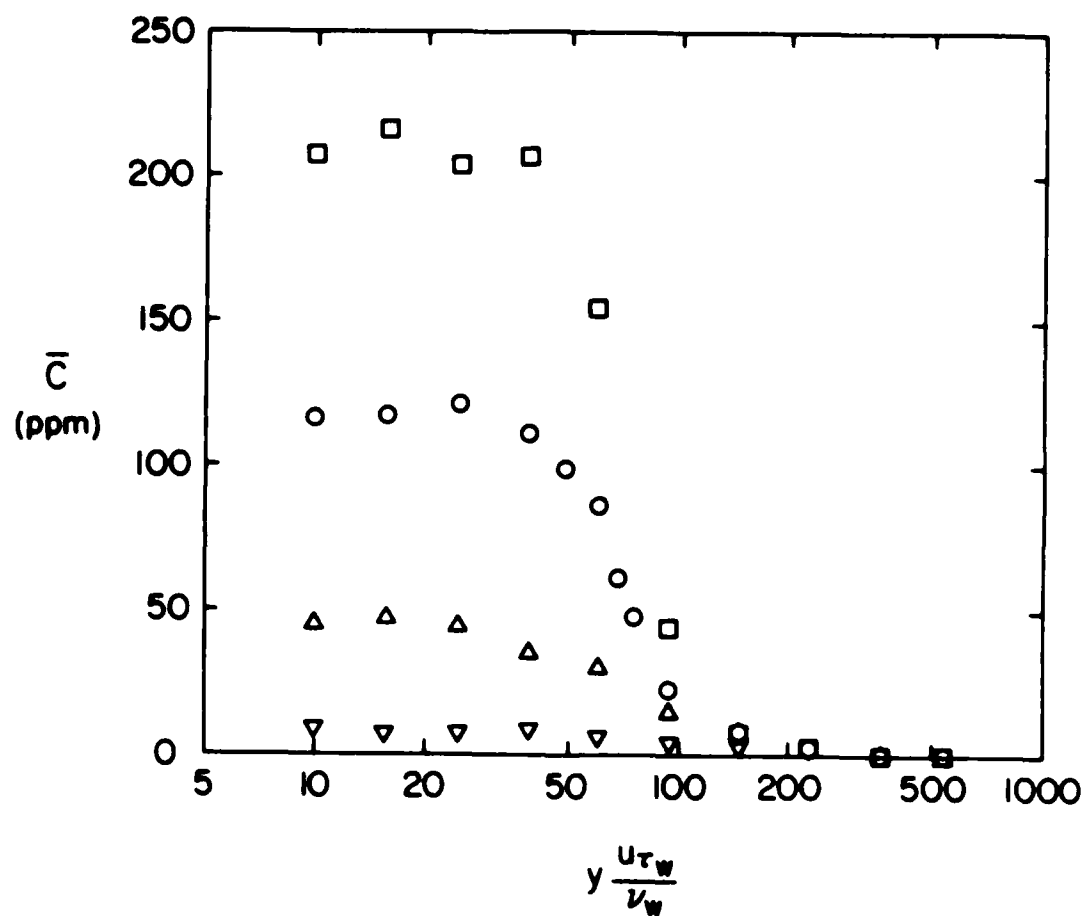
Figure 5.   Mean polymer concentration profiles downstream of injector; □, x/h = 4; ○, 8; △, 16; ▽, 32.

Turbulence statistics are usually presented normalized with the local values of the shear velocity and kinematic viscosity. For a Newtonian flow this normalization results in "universal" behavior of turbulence statistics in the near-wall region. Similar universality has not been demonstrated for even fully developed drag-reducing flows. Hence, this normalization does not provide a basis for comparison and tends to obscure the absolute changes in the statistical quantities.

An absolute measure of the effect of the injected polymer solution on the structure of the flow results from comparing the turbulence statistics of the injected flow with those of the water flow at the same physical location. The following figures show the changes in structure by presenting the ratio of a given quantity for the drag-reducing flow to the corresponding quantity for the same physical location in the water flow with no injection.

Figure 8 shows the fractional change in the mean streamwise velocity, $\overline{U}$, with polymer injection from that of the water flow as a function of distance normal to the wall for the four streamwise measurement locations. The distance from the wall, y_w^+, is normalized with the shear velocity and kinematic viscosity of the water flow for reference only and is not meant to imply that the flow structure should be correlated by this normalization. The mean velocity decreased in the high polymer concentration near-wall region, y_w^+ less than one hundred. The effect is most pronounced in the near-injector location where the polymer concentration is highest and diminishes with increasing streamwise distance. A slight acceleration of the outer flow results from mass conservation considerations.
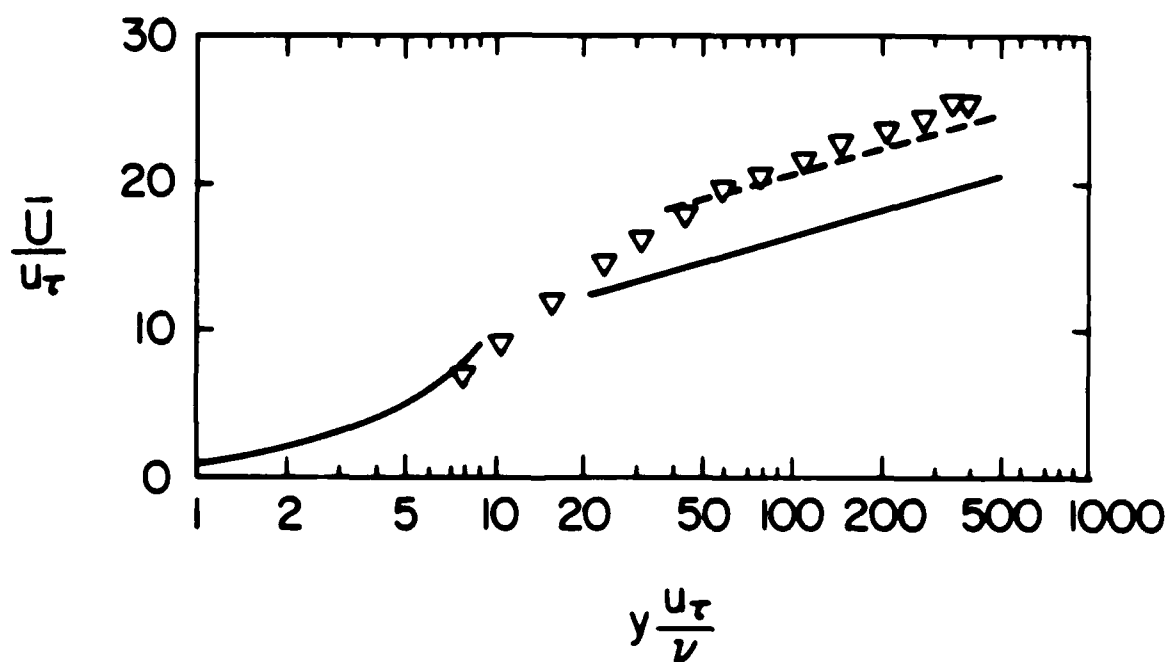
Figure 6.   Mean velocity profile at x/h = 32 for polymer injection (34 percent drag reduction); ———, water flow; - - - -, Luchik (1985) (31 percent drag reduction).
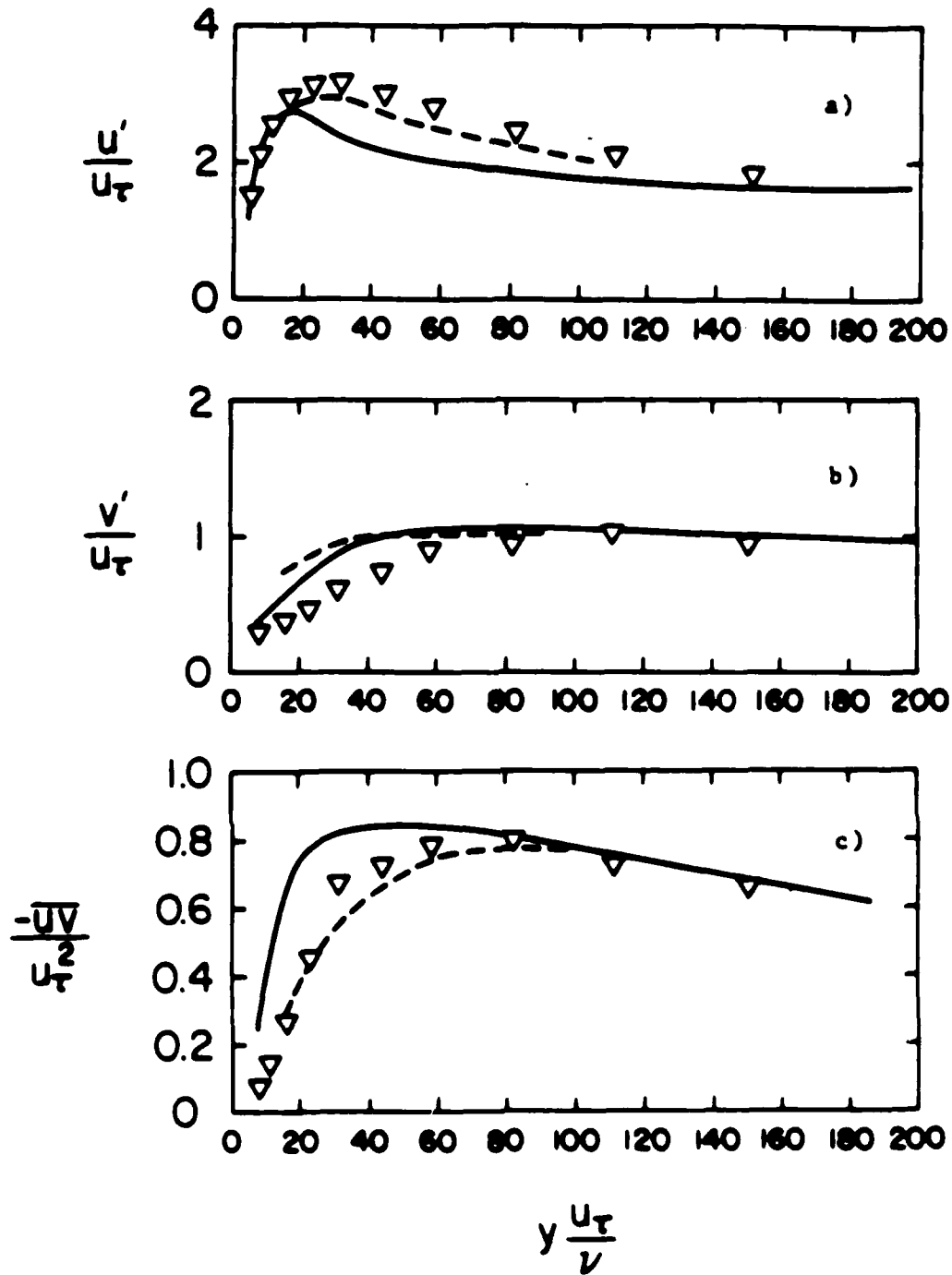
Figure 7. Turbulence statistics profiles at x/h = 32 for polymer injection (34 percent drag reduction). a) RMS of streamwise velocity; b) RMS of normal velocity; c) turbulent shear stress; ———, water flow; - - - -, Luchik (1985) (31 percent drag reduction).
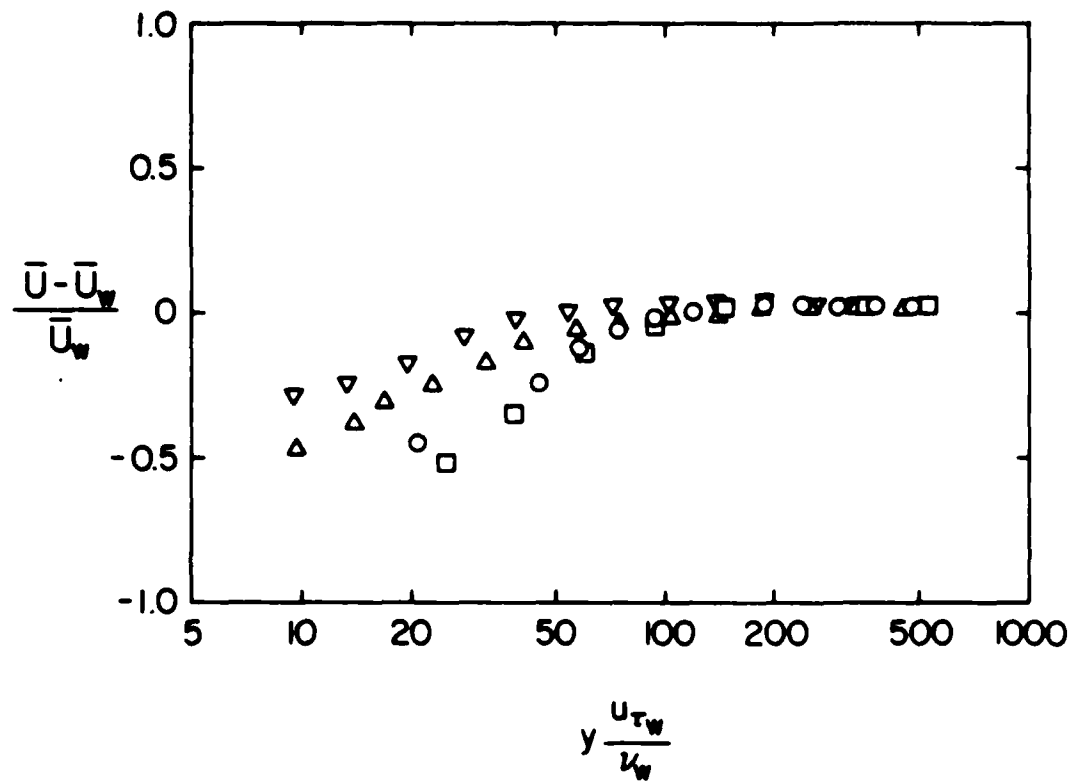
Figure 8. Fractional change in streamwise velocity with polymer injection; □, x/h = 4; , 8; △, 16; ▽, 32.

The fractional change in the root-mean-square (RMS) of the streamwise velocity, u′, (Figure 9) exhibits similar behavior for y_w^+ less than thirty but shows an increase for y_w^+ from thirty to two hundred. The decrease immediately adjacent to the wall and the increase further from the wall can be attributed to a corresponding decrease and increase in the gradient of $\overline{U}$ in these regions. Figure 10 shows the behavior of the RMS of the normal velocity, v′, for the four measurement locations during polymer injection. There is a decrease in v′ across the entire channel at all streamwise locations except x/h=4. At this location, v′ is reduced only in the high concentration near-wall region and appears to be unaltered in the outer flow.

The fact that the turbulent shear stress, $\overline{uv}$, approaches zero at the channel centerline makes comparison of this quantity in a similar manner somewhat more ambiguous. For this reason, the comparison is made by plotting the measured value of $\overline{uv}$ for the injected flow versus distance from the wall along with a line representing $\overline{uv}$ for the fully developed water flow. These data are presented in Figure 11 where both quantities are normalized with the shear velocity of the water flow. In a manner similar to that of v′, the value of $\overline{uv}$ is reduced across the entire channel height at all locations except at x/h=4. Here the value off $\overline{uv}$ deviates significantly from that of the water flow only in the region of high polymer concentration.

2.3 Conclusions and Recommendations

From these data several general results can be identified. The structure of the near wall region, y_w^+ less than one hundred, appears to be highly dependent upon the polymer concentration. The mean streamwise velocity gradient is decreased
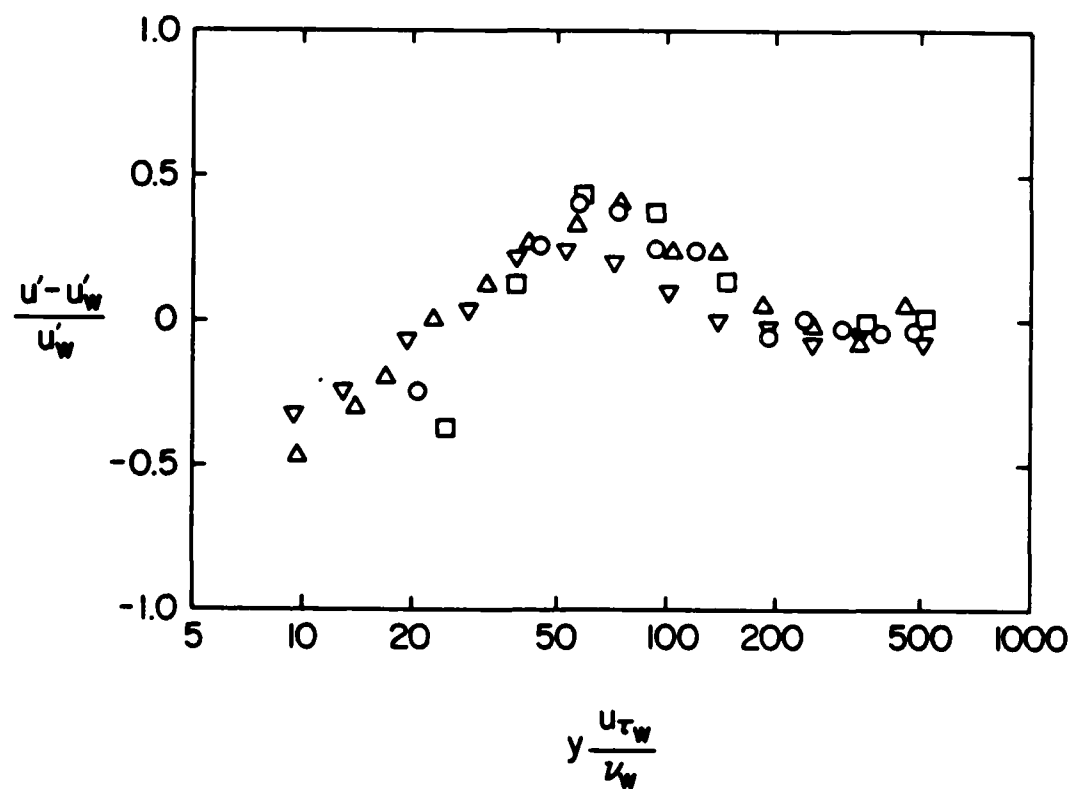
Figure 9.   Fractional change in the RMS of the streamwise velocity
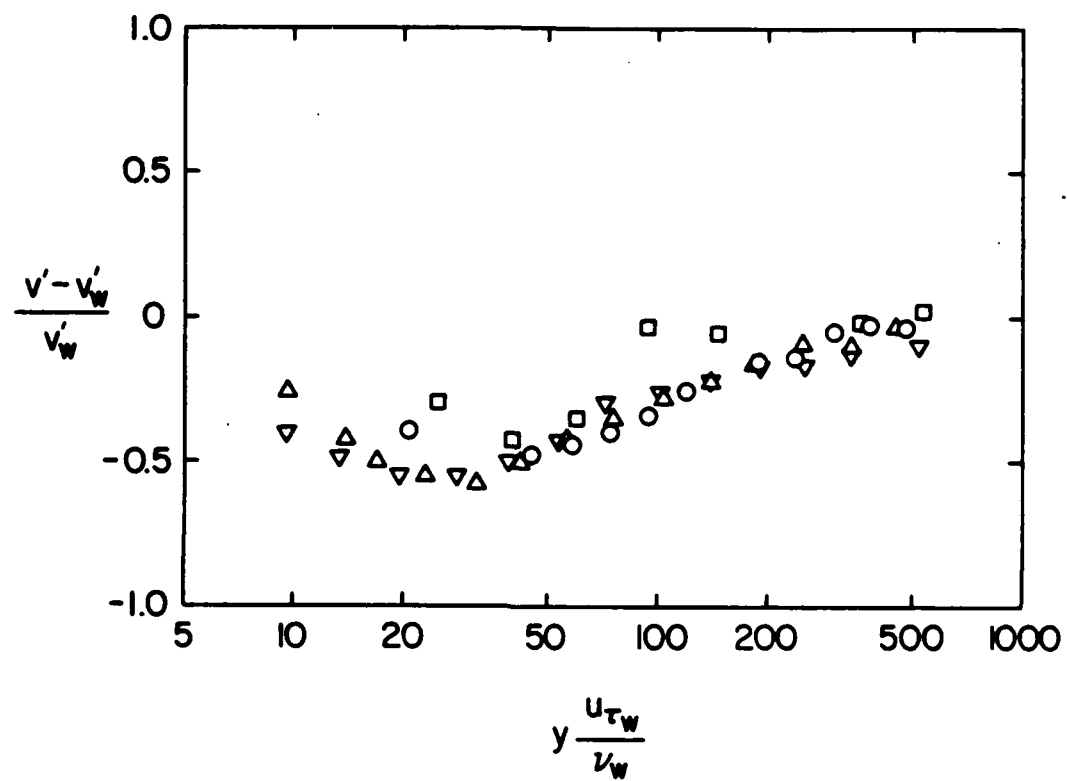with polymer injection; □, x/h = 4; ◯, 8; △, 16; ▽, 32.

Figure 10.   Fractional change in the RMS of the normal velocity with polymer injection; $\square$, $x/h = 4$; $\bigcirc$, 8; $\triangle$ 16; ∇, 32.
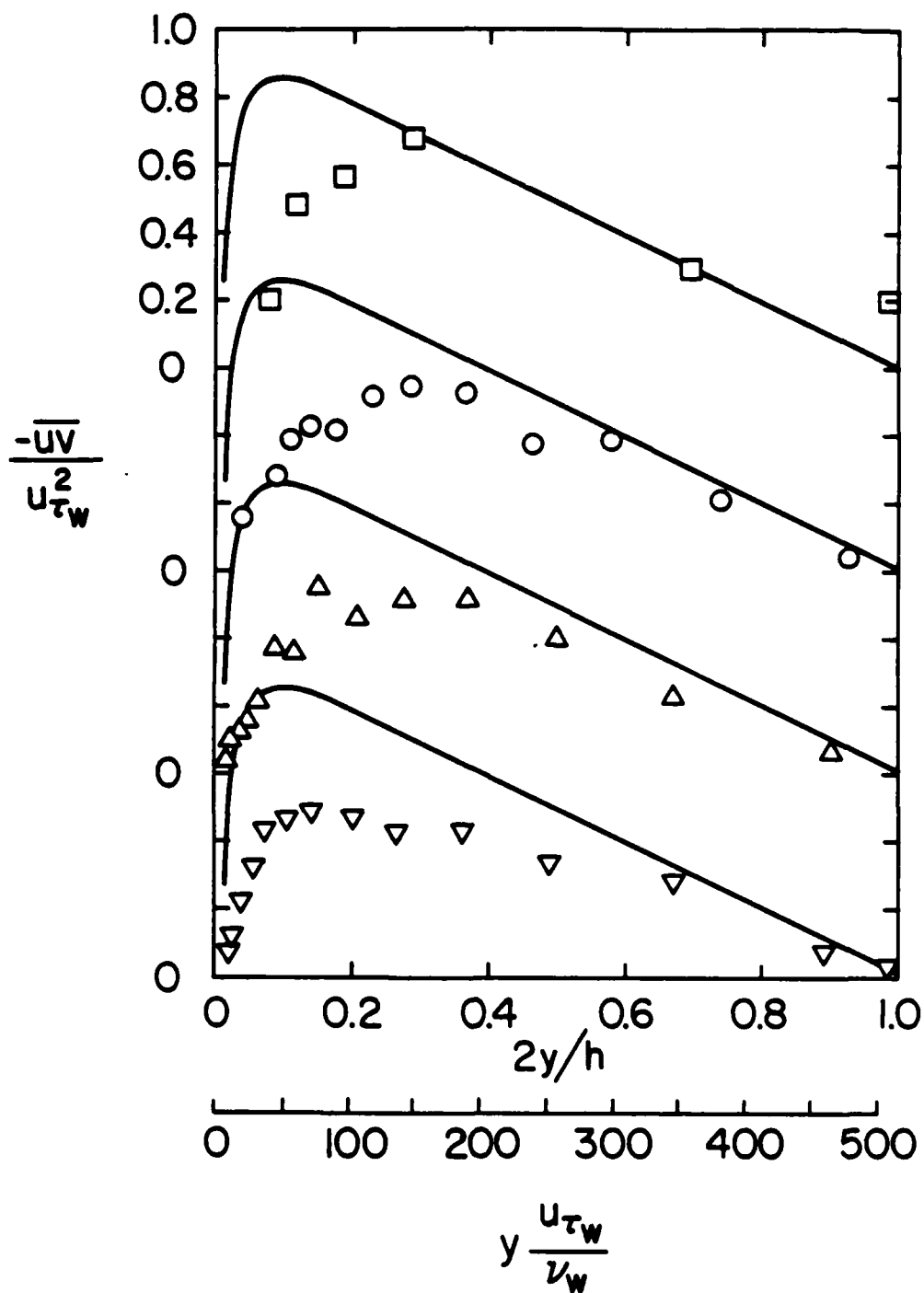
Figure 11.   Reynolds stress profiles for flow with polymer injection; □,
x/h = 4; ◯, 8; △, 16; ▽, 32; ——, water flow.

immediately adjacent to the wall and increased at distances further from the wall. This results in a corresponding decrease and increase in u' relative to the same location in the water flow. The RMS of the normal velocity and the turbulent shear stress are always less than or equal to the values for the water flow. At x/h = 4, these quantities deviate greatly from the corresponding water flow levels only in the high-concentration layer. Further downstream, where the polymer is present across the entire channel height, v' and $\overline{uv}$ are reduced everywhere. This indicates that once the polymer has mixed beyond the wall region in even small quantities the structure of the flow has been altered in every aspect.

Since the spanwise average of the dye concentration across the channel was not constant with time, the attenuation method cannot be used to deduce instantaneous values of the polymer concentration (see Tiederman et al., 1986). Instead, time-resolved concentration measurements will be made using the fluorescent dye technique of Koochesfahani and Dimotakis (1986). One objective of our future efforts will be to measure directly the product of the normal velocity fluctuation, v and the polymer concentration fluctuation, c'. The time average of this product is the additional unknown in the Reynold's averaged equation for polymer concentration.

The sharp gradients of the average polymer concentration imply that even sharper gradients exist instantaneously. Future efforts should focus on this high Schmidt number mixing in the near-injector region.

3. NEWTONIAN BURST FREQUENCY

The objective of this experiment was to confirm the extrapolation made by Luchik and Tiederman (1987) that the average time between bursts, $\overline{T}_B$ (the inverse of the burst frequency) scales with inner variables for Newtonian, fully developed channel flows. Specifically the proposed relationship is

$$\overline{T}_B^+ = \frac{\overline{T}_B\, u_r^2}{\nu} = 90 \tag{2}$$

for Reynolds numbers $\geq 10,000$.

3.1 Apparatus and Procedures

The experiments were conducted in the $2.5 \times 25.0\ cm$ channel and flow loop described in Section 2.1. No fluid was injected through the slots and the water was circulated at the maximum flow-rate capacity using all four pumps. For this situation the Reynolds number based on the average flow rate and channel height, h=2.5 cm, was nominally 50,000.

Streamwise velocity measurements were made at $y^+=30$ by operating the laser velocimeter on the green line (514.5 nm) in a one-component, dual beam configuration. This one-component configuration was chosen because it was clear prior to the experiments that it would be difficult to achieve data rates equal to or greater than the viscous frequency ($u_r^2/\nu = 8,800\ Hz$) with a spanwise probe volume length $z^+ \leq 20$. These constraints on data rate and probe volume length were suggested previously by Bogard and Tiederman (1986) and Luchik and Tiederman (1985, 1987). Since all high

Reynolds number laser velocimeter measurements are limited by these constraints, data were also acquired with a larger probe volume and a slower sampling frequency in an effort to define these constraints more precisely.

All of the water in the flow loop was seeded uniformly with 2.02 μm diameter, white, latex spheres. These scattering particles were chosen because their specific gravity is nearly 1.0 and the fringe spacing of the laser velocimeter was 2.68 μm.

The receiving optics were aligned to receive forward scattered light at an angle of either $0\degree$ or $45\degree$ with respect to the optical axis of the transmitting optics. At $45\degree$, the probe volume length was truncated to a spanwise length given by $z^+ = 21$. At $0\degree$, the probe volume length was $z^+ = 137$.

Measurements were made with the $45\degree$ configuration at particle number densities that produced nominal data rates of 4 kHz and 8 kHz. The receiving optics were then realigned to $0\degree$ and the particle density was adjusted to produce an 8 kHz data rate. After collecting and storing data from the free-running counter processor, the velocity records were then sampled at equal intervals of time corresponding to their respective data collection rates using linear interpolation between data points.

The techniques for grouping single-component velocity detections of ejections into burst detections as presented by Luchik and Tiederman (1987) were used in this study. In particular the u-level, modified u-level and VITA algorithms were used to detect ejections. The u-level method has one threshold parameter, L, and a detection occurs when the fluctuation, u, about the mean $\overline{U}$ is given by

$$u \leq -L \; u' \qquad (3)$$

Here u' is the root-mean-square of u. For the modified u-level technique Equation 3 describes the condition when the detector is turned "on." A modified u-level detection ends when

$$u > -0.25 \; L \; u' \qquad (4)$$

The threshold for a VITA detection is given by

$$VAR > k \; u'^2 \qquad (5)$$

where

$$VAR = \tilde{U}^2 - \tilde{U}^2 \qquad (6)$$

and

$$\tilde{U} = \frac{1}{T_A} \int_{t-\frac{1}{2}T_A}^{t+\frac{1}{2}T_A} U \; d \; t \qquad (7)$$

The value for T_A was chosen to yield the maximum number of detections independent of threshold. Ejections are then grouped into burst detections by using the probability functions for time between ejections to estimate a time period, τ_E, that separates ejections from the same burst from ejections from other bursts. If the time between temporally adjacent ejections is less than τ_E, those two ejections are considered to be part of one burst. Conversely if the time between adjacent ejections is larger than τ_E, then those two ejections are from different bursts.

3.2 Results

Figure 12 which is a plot of the probability that $T > T_E$ demonstrates the procedure for determining τ_E for u-level detections. This is the same technique used by Barlow and Johnston (1985) and Luchik and Tiederman (1987) for quadrant 2 detections from two-component data. As indicated by the different symbols on Figure 13, the value of τ_E varied somewhat with specification of the threshold L. The u-level method yields an average time between bursts, $\overline{T}_B$, of 8.0 ms for the data set where $z^+ = 21$ and the sampling data rate equals 8 kHz.

The u-level and quadrant 2 procedure for determining τ_E does not work for either modified u-level or VITA detections. The procedure of leaving the detector "on" in the modified u-level method and the integration time, T_A, in the VITA method effectively low-pass filter the velocity record. As a result both methods, by design, do not detect all of the ejections from the same burst. Consequently the probability function is reduced substantially for small values of time between ejections, T_E, while it is unaffected at large values of T_E. Consequently, a method based on fitting the histogram of the number of ejections, N_E, in a small interval of T_E to a Poisson distribution was used to determine τ_E.
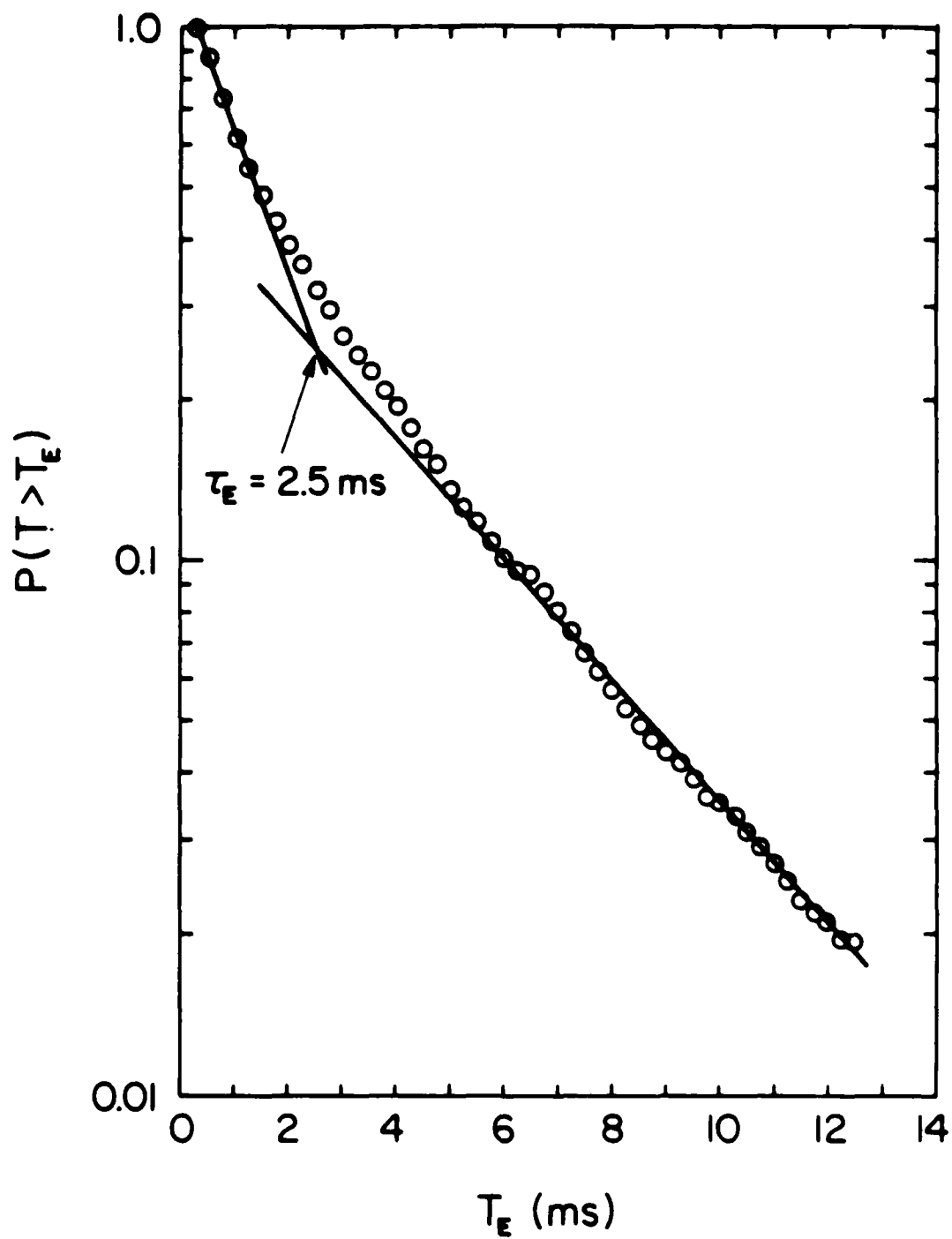
Figure 12.   Probability function for time between ejections using
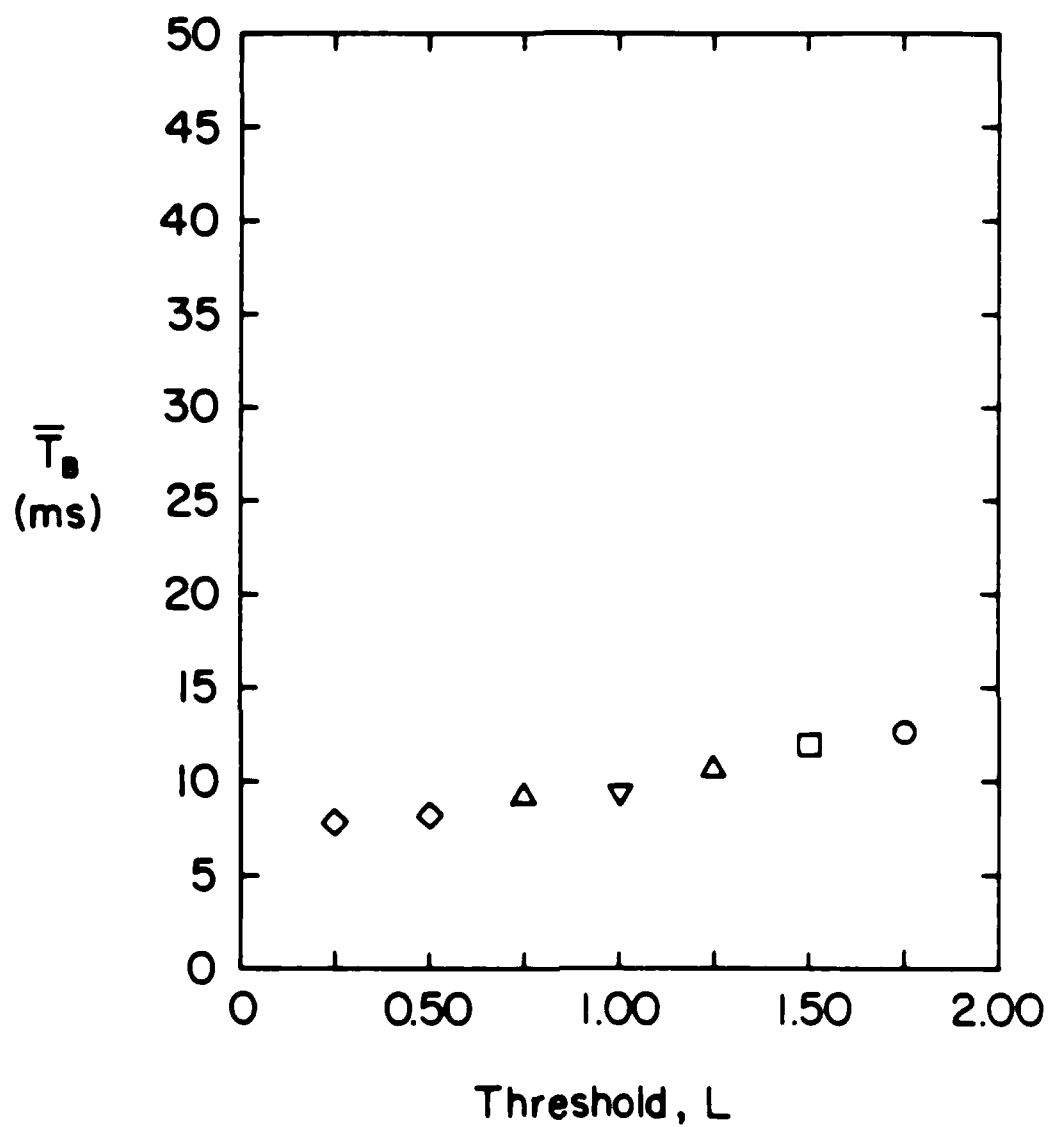u-level detection; $z^+ = 21$, 8 kHz data.

Figure 13.   Time between bursts for u-level method;
◇, $\tau_E = 2.5$ ms; △, $\tau_E = 2.7$ ms; ▽, $\tau_E = 2.6$ ms; □,
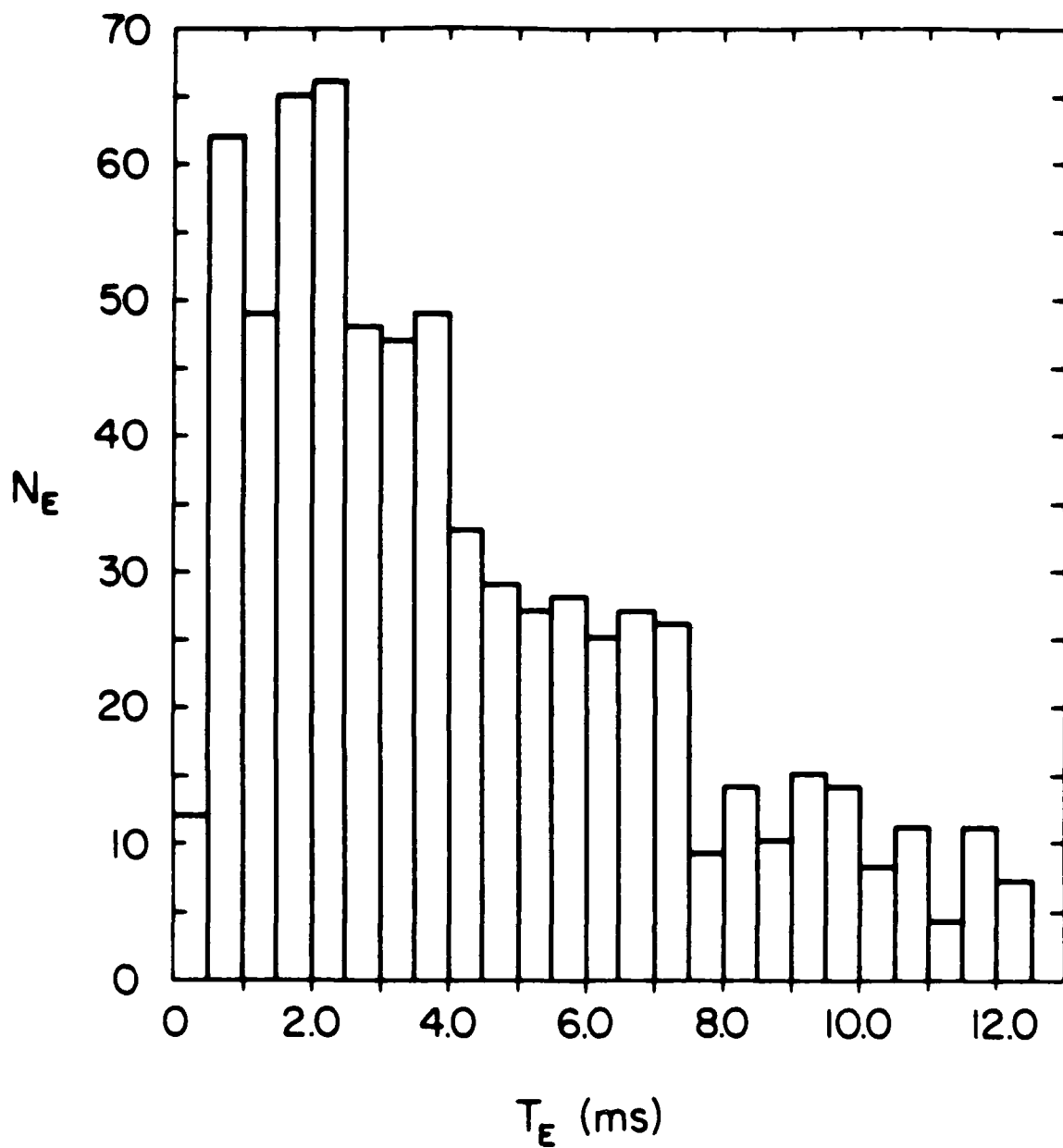$\tau_E = 2.4$ ms;   , $\tau_E = 2.1$ ms.

Figure 14.   Histogram of time between ejections for modified u-level detections; $z^+ = 21$, 8 kHz data.

In practice this procedure for matching the experimental histogram, shown in Figure 14, to the theoretical distribution is dependent upon the investigators choice of "bin" size which in this case is the interval in T_E. If the interval is too small the histogram does not approximate a smooth curve while if the interval is too large the method has poor resolution. With several hundred ejection detections, a good compromise is to choose a time interval which places the mode in the fourth or fifth bin. The mode of this experimental distribution is then set equal to the mean value of the Poisson distribution and τ_E is chosen to be the value of T_E where $P(T \leq T_E) = 0.95$ for the Poisson distribution.

An illustration of the grouping technique for modified u-level detections is shown in Figure 15. This short segment of the data record was chosen because it contains examples where the method worked well as well as examples where it may not have properly grouped detections. For example, based on the u signal, the group of 3 ejections between 170 and 175 ms are most likely one burst. On the other hand the two ejections between 156 and 160 ms are most likely from different bursts because the streamwise velocity is so much larger than the mean value in the interval between the detections. We did not expect these simple grouping methods to be perfect. Undoubtedly additional criteria could be developed that would improve the precision of the grouping. At present the uncertainty that propagates to the determination of $\overline{T}_B$ is probably on the order of 20%. Despite this uncertainty, which is common to all statistical methods for estimating τ_E, the modified u-level method yields a value of $\overline{T}_B = 12.0$ ms over a rather wide range of threshold levels for the $z^* = 21$, 8 kHz data (see Figure 16).

The Poisson method for estimating τ_E must also be used when the ejections are detected using the VITA method. As shown in Figure 17, the procedure yields $\overline{T}_B = 10.0$ over a small but finite range of the threshold parameter, k, for the $z^* = 21$, 8 kHz data.

The average value of $\overline{T}_B$ from the three different methods used to analyze the $z^* = 21$, 8 kHz data was 10.0 ms. The same three methods were applied to the $z^* = 21$, 4 kHz data set and the $z^* = 137$, 8 kHz data set. It was more difficult to determine τ_E for these data sets because some temporal resolution was missing from the 4 kHz data and some spatial averaging occurred in the $z^+ = 137$ data. These "degradations" mean that some ejections are not detected by the procedures and this affects plots such as those on Figures 12 and 14. Nonetheless estimates were made using all three methods and the average value of $\overline{T}_B$ for these two additional data sets are reported in the nondimensional plots that show the variation of $\overline{T}_B$ with Reynolds number.

Figures 18, 19, and 20 show how the present data along with previous data (Luchik and Tiederman, 1987) scale with Reynolds number. All of these results were obtained in the 2.5 × 25.0 cm channel. The outer scaling of $\overline{T}_B$ using the center-line velocity, U_0, and channel half-height, $h/2$, clearly does not yield a constant nondimensional value. Neither does the mixed scaling proposed by Alfredsson and Johanssen (1984). Scaling $\overline{T}_B$ with inner variables does work yielding
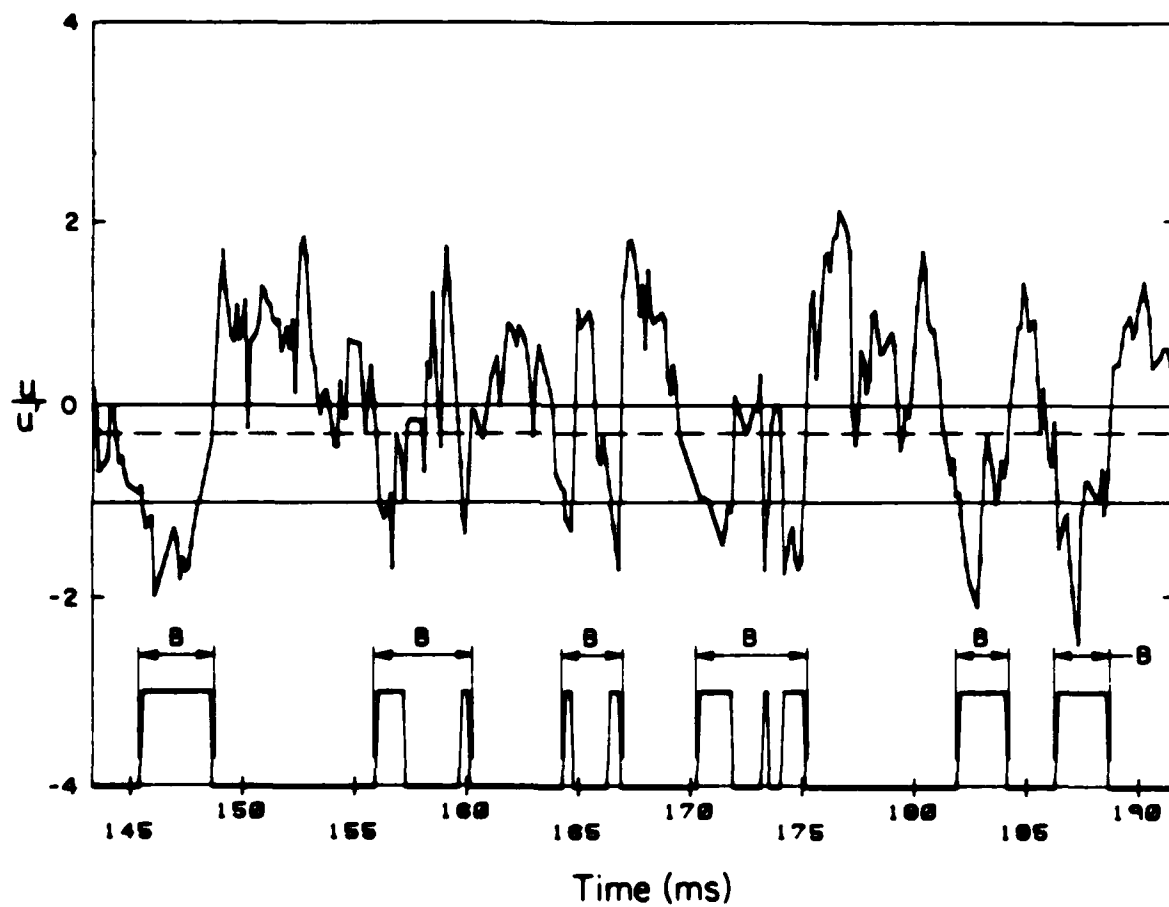
$$\overline{T}_B^* = 90$$

Figure 15. Illustration of modified u-level detections and subsequent grouping into burst events.
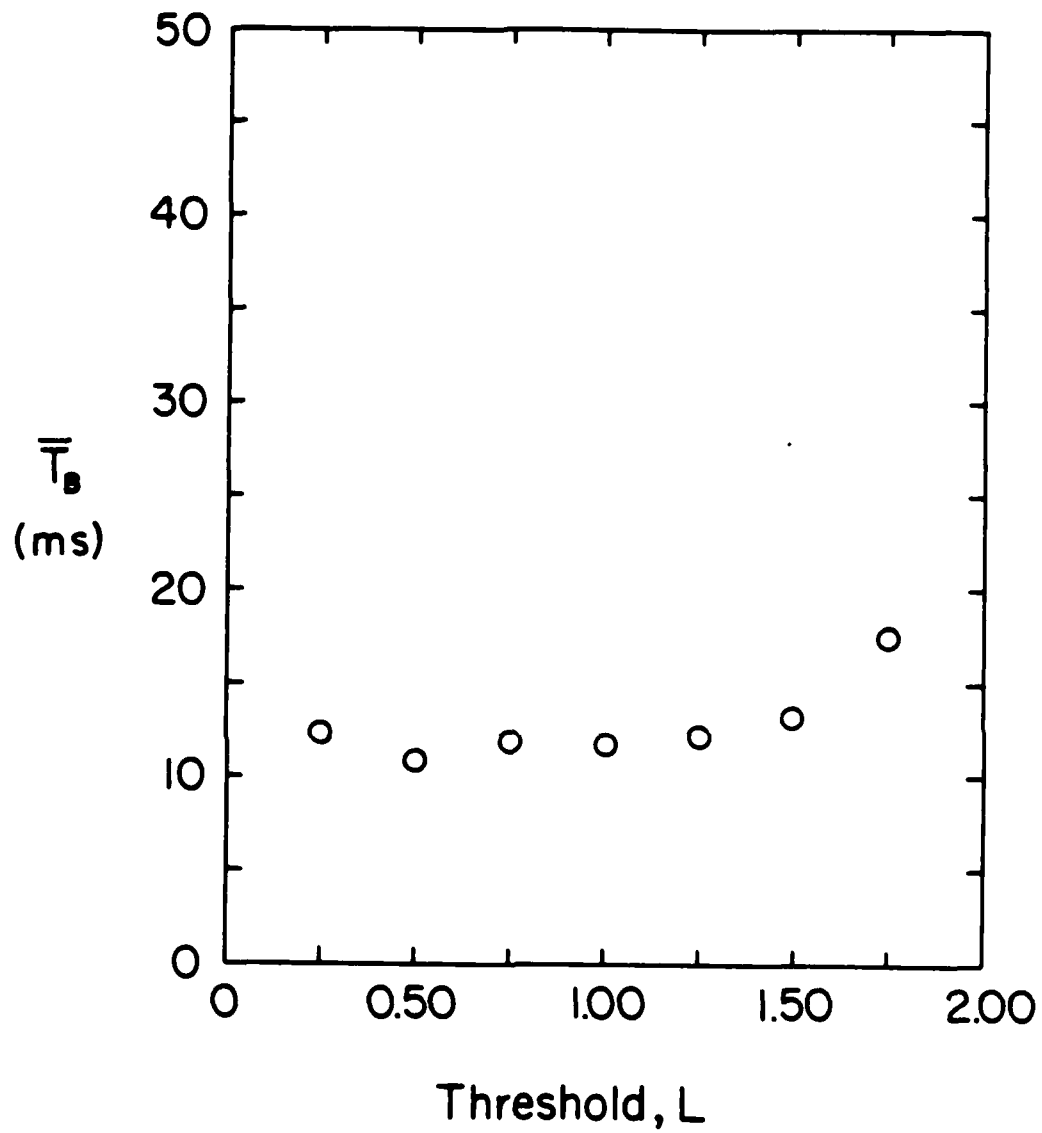
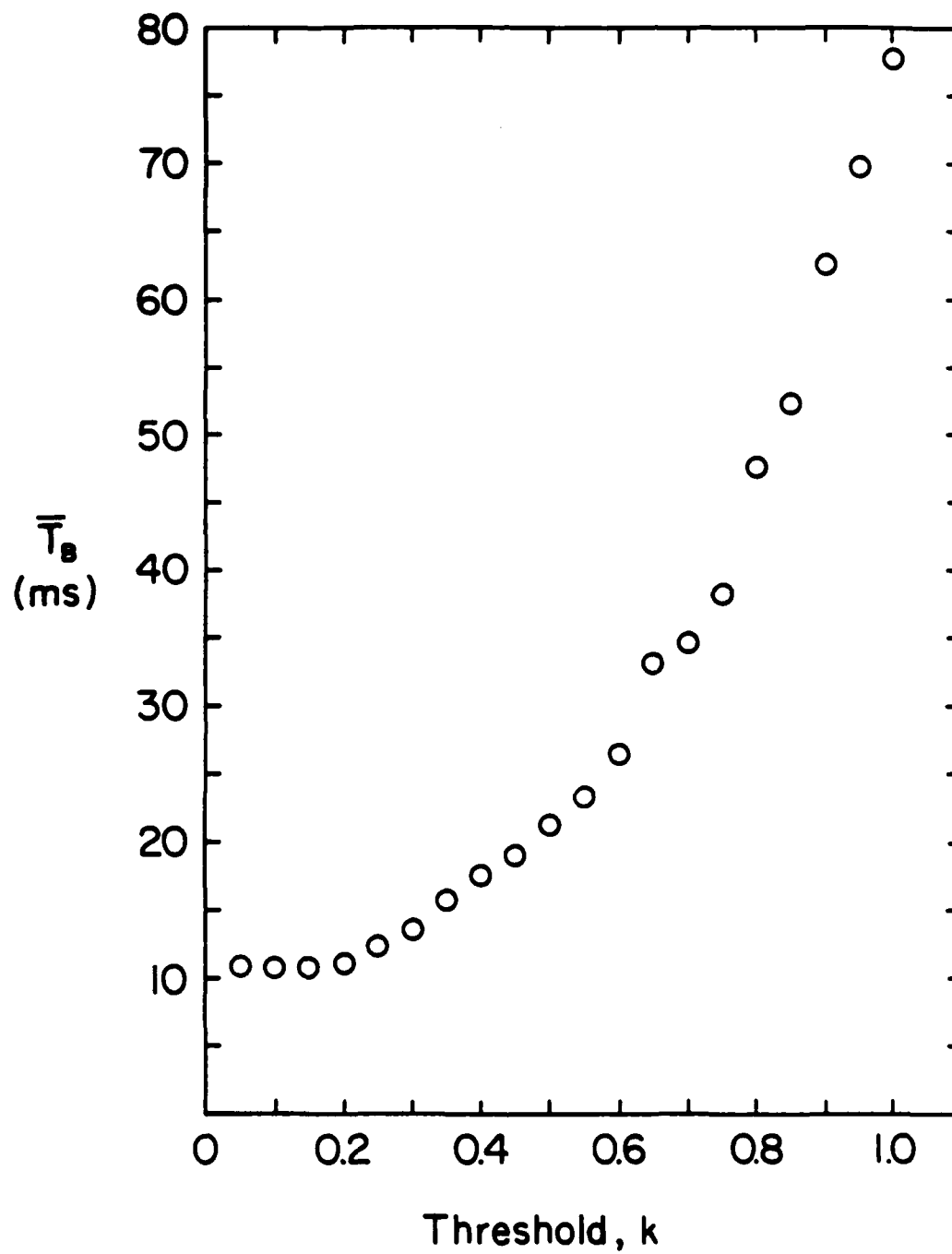Figure 16.   Time between bursts for modified u-level method.

Figure 17.   Time between bursts for VITA method.

3.3 Conclusions

The principal conclusion is that $\overline{T}_B^+ = 90$ for $9{,}400 \leq \mathrm{Re}_h \leq 50{,}000$ in a fully developed channel flow. Based on our experience with data from longer spanwise probe volumes and with data rates less than the viscous frequency, it is recommended that the probe volume have a spanwise length of $z^+ \leq 20$ and that the data rate be equal or greater than the viscous frequency, u_r^2/ν.
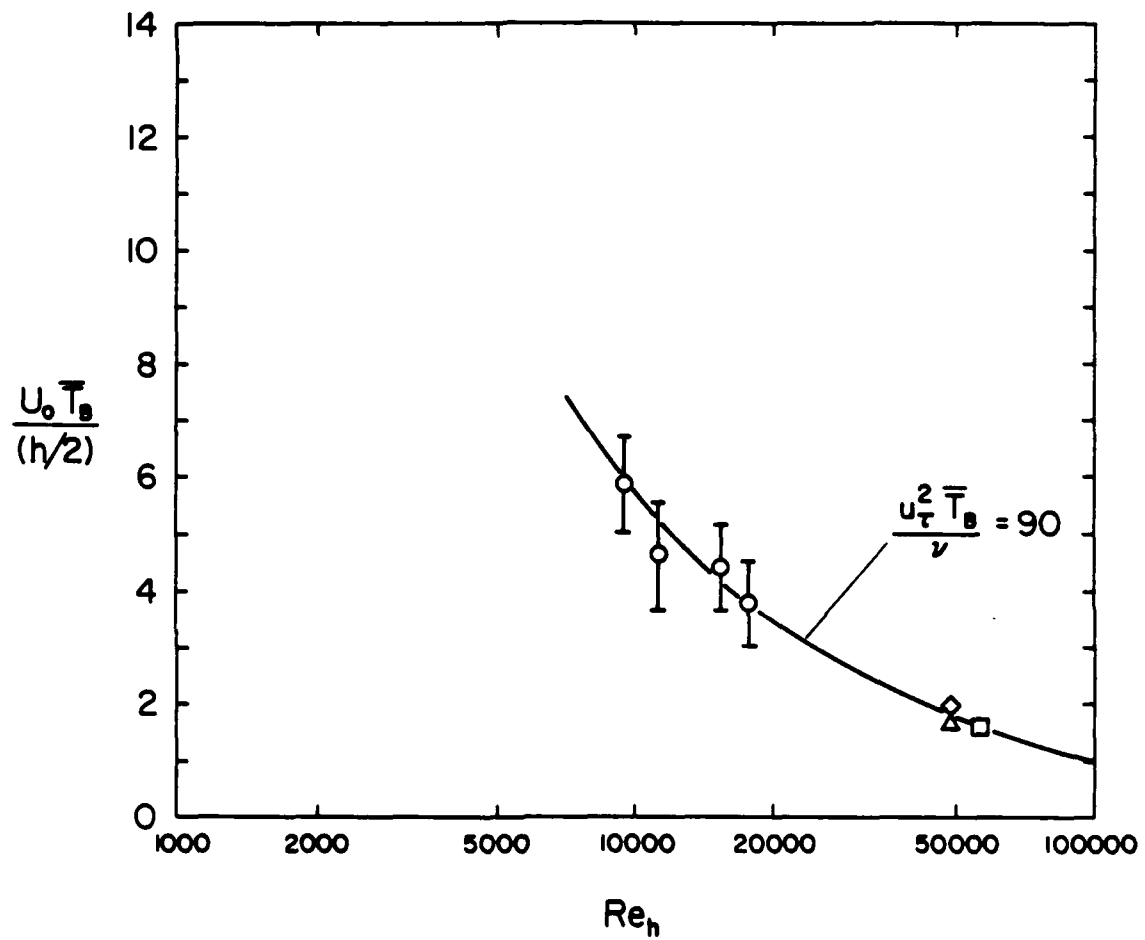
Figure 18. Outer scaling for time between bursts; ◯, Luchik & Tiederman (1987); , $z^+ = 21$, 4 kHz; △, $z^+ = 21$, 8 kHz; □, $z^+ = 137$, 8 kHz.
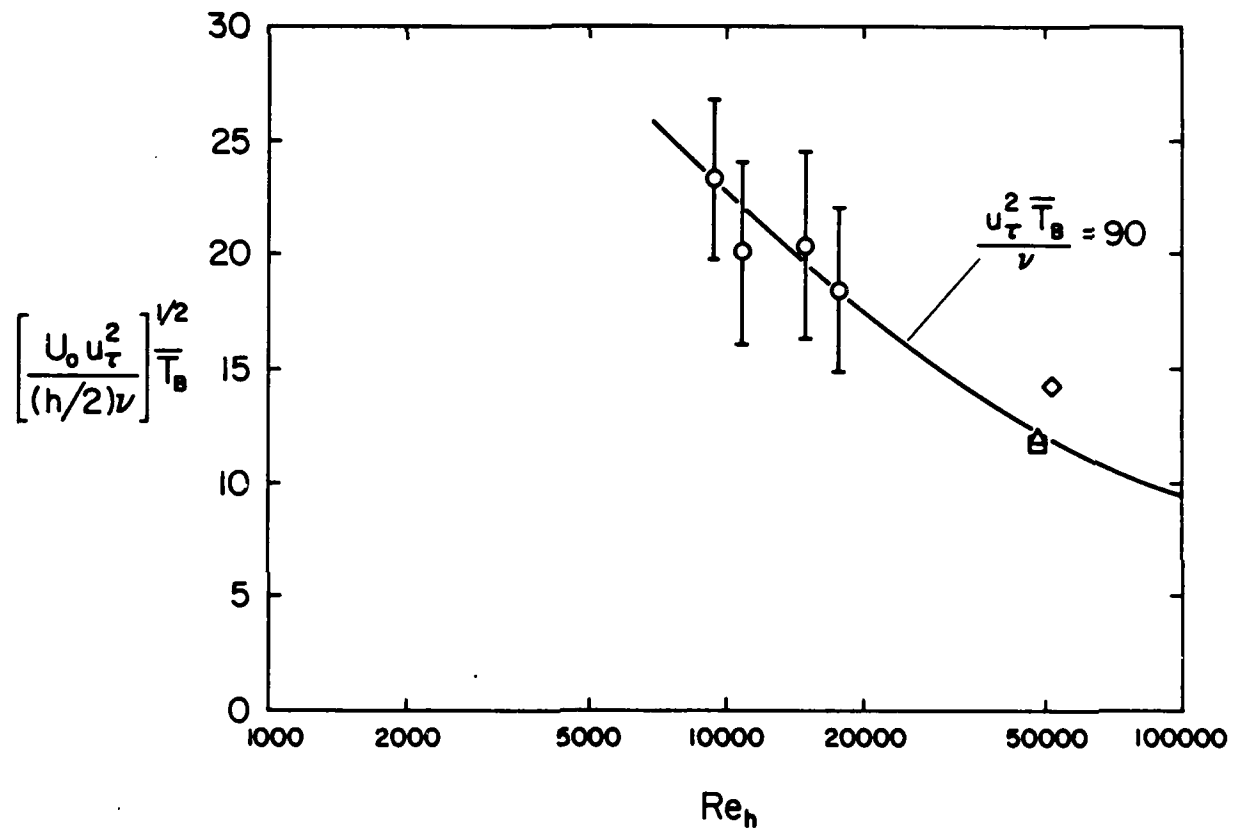
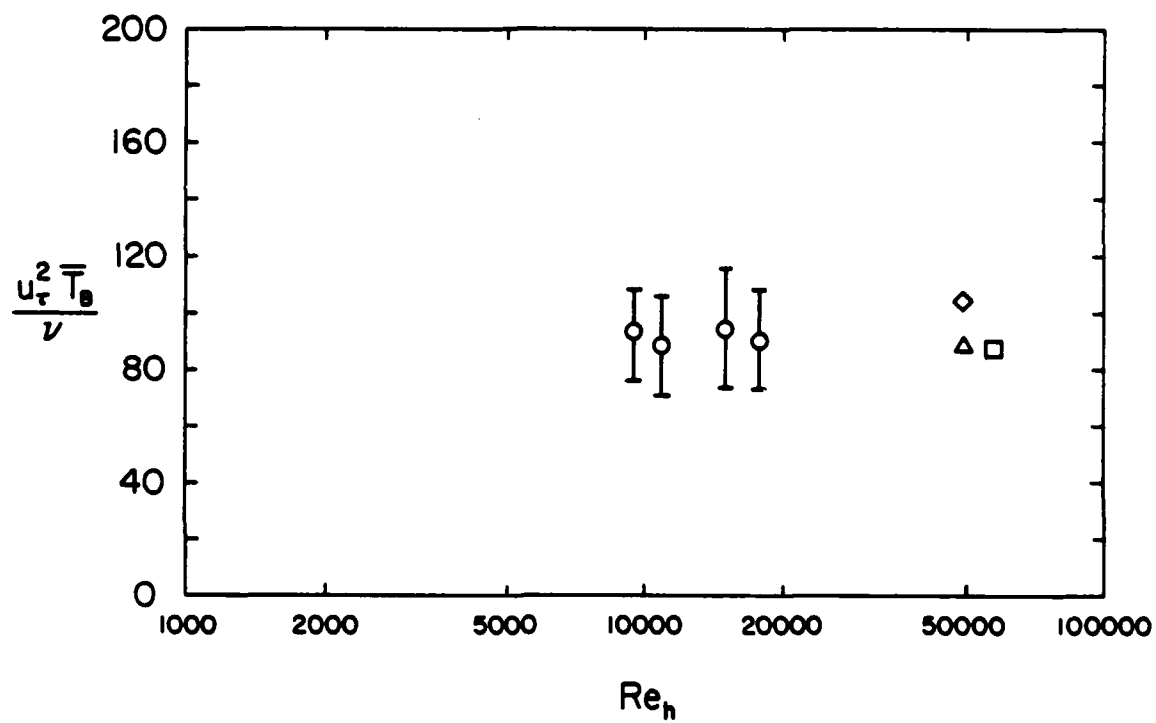Figure 19.   Mixed scaling of time between bursts (see Figure 18 for symbols).

Figure 20. Inner scaling of time between bursts (see Figure 18 for symbols).

4. REFERENCES

Alfredsson, P.H. and A.V. Johanssen, 1984. Time scales in turbulent channel flow. *Phys. Fluids, 27*, 1974.

Barlow, R.S. and J.P. Johnston, 1985. Structure of turbulent boundary layers on concave surfaces. Report MD-47, Thermosciences Division, Department of Mechanical engineering, Stanford University; Stanford, California.

Berman, N.S., 1985. Velocity fluctuations in non-homogeneous drag reduction. *Chem. Engr. Commun., 42*, 37.

Bewersdorff, H.-W., 1985. Heterogeneous drag reduction in turbulent pipe flow. *The Influence of Polymer Additives on Velocity and Temperature Fields,* B. Gampert, ed., Springer-Verlag, Berlin.

Corino, E.R. and R.S. Bradkey, 1969. A visual investigation of the wall region in turbulent flow. *J. Fluid Mech., 37*, 1.

Frings, B., 1985. ¯Annular injection of concentrated polymer solutions into the wall region of a turbulent pipe flow. *The Influence of Polymer Additives on Velocity and Temperature Fields,* B. Gampert, ed., Springer-Verlag, Berlin.

Kim, H.T., S.J. Kline and W.C. Reynolds, 1971. The production of turbulence near a smooth wall in a turbulent boundary layer, *J. Fluid Mech, 50*, 133.

Koochesfahani, M.M. and P.E. Dimotakis, 1986. Mixing and chemical reactions in a turbulent mixing layer. *J. Fluid Mech, 170*, 83.

Luchik, T.S., 1985. The effect of drag reducing additives on turbulent structure in channel flow. Ph.D. Thesis, Purdue University.

Luchik, T.S. and W.G. Tiederman, 1985. Effect of spanwise probe volume length on laser velocimeter measurements in wall bounded turbulent flows. *Exp. in Fluids, 3*, 339.

Luchik, T.S. and W.G. Tiederman, 1987. Timescale and structure of ejections and bursts in turbulent channel flows. *J. Fluid Mech., 174*, 529.

Tiederman, W.G., 1979. Interpretation of laser velocimeter measurements in turbulent boundary layers and regions of separation. *Turbulence in Liquids,* J.L. Zakin and G.K. Patterson, eds., University of Missouri-Rolla, 173.

Tiederman, W.G., D.T. Walker, T.S. Luchik and A. Abdallah, 1986. Injection of drag reducing additives into turbulent water flows: Techniques for concentration measurements and Reynolds number scaling. Report PME-FM-86-1, School of

Mechanical Engineering, Purdue University, West Lafayette, Indiana.

Walker, D.T., W.G. Tiederman and T.S. Luchik, 1986. Optimization of the injection process for drag reducing additives. *Exp. in Fluids, 4,* 114.

5. PUBLICATIONS AND PRESENTATIONS

Publications

1. Luchik, T.S. and W.G. Tiederman, "Time scale and structure of ejections in turbulent channel flow," *Journal of Fluid Mechanics, 179,* pp. 1-19, 1987.

Presentations

1. W.G. Tiederman, "Turbulent Burst Detections at High Reynolds Number," 39th Annual Meeting of the Division of Fluid Dynamics, American Physical Society, Columbus, Ohio, November 25, 1986.

2. W.G. Tiederman, "Turbulent Burst Detections," Fluid Mechanics Seminar, School of Mechanical Engineering, Purdue University, West Lafayette, Indiana, December 5, 1986.

6. DISTRIBUTION LIST

Dr. Michael M. Reischman, Code 1132F
Office of Naval Research
800 North Quincy Street
Arlington, VA 22217

Defense Technical Information Center
Building 5, Cameron Station
Alexandria, VA 22314
(12 copies)

Office of Naval Research
Resident Representative
536 S. Clark Street, Rm. 286
Chicago, IL 60605-1588

Mechanical Engineering Business Office
Purdue University
West Lafayette, IN 47907

Director
Naval Research Laboratory
Attn: Code 2627
Washington, DC 20375
(6 copies)

Professor D.G. Bogard
Department of Mechanical Engineering
The University of Texas
Austin, TX 78712

Dr. O. Kim, Code 6124
Naval Research Laboratory
Washington, DC 20375

Dr. Steve Deutsche
ARL
Pennsylvania State University
P.O. Box 30
State College, PA 16801

Professor S.J. Kline
Thermosciences Division
Department of Mechanical Engineering
Stanford University
Stanford, CA 94305

James H. Green, Code 634
Naval Ocean System Center
San Diego, CA 92152

G. Leal
Department of Chemistry and
    Chemical Engineering
California Institute of Technology
Pasadena, CA 91125

Professor T.J. Hanratty
Department of Chemical Engineering
1209 West California Street
Box C-3
Urbana, IL 61801

Justin H. McCarthy
Code 1540
David Taylor Naval Ship R&D Center
Bethesda, MD 20084

Dr. R.J. Hansen, Code 5844
Naval Research Laboratory
Washington, DC 20375

Professor E.W. Merrill
Department of Chemical Engineering
Massachusetts Institute of Technology
Cambridge, MA 02139

Dr. J.H. Haritonidis
Room 37-461
Massachusetts Institute of Technology
Cambridge, MA 02139

Dr. D.L. Hunston
Polymer Sciences & Standards Division
National Bureau of Standards
Washington, DC 20234

Mr. G.W. Jones
Code 55W3
Naval Sea Systems Command
Washington, DC 20362

Dr. John Kim
M.S. 202A-1
NASA - Ames Research Center
Moffett Field, CA 94035

Dr. T.E. Pierce
Code 63R31
Naval Sea Systems Command
Washington, DC 20362

Steve Robinson
M.S. 229-1
NASA - Ames Research Center
Moffett Field, CA 94035

Professor W.W. Willmarth
Department of Aerospace Engineering
University of Michigan
Ann Arbor, MI 48109

END

7-87

DTIC